ACS APPLIED MATERIALS & INTERFACES

Research Article

www.acsami.org

Thermal Properties of the Stationary Current in Mesoporous Pt/TiO_2 Structures in an Oxyhydrogen Atmosphere

M. A. Hashemian,[†] E. Palacios,[†] I. I. Nedrygailov,[‡] D. Diesing,[‡] and E. G. Karpov*,[†]

[†]Civil & Materials Engineering, University of Illinois, Chicago, Illinois 60607, United States

[‡]Fakultät für Chemie, Universität Duisburg–Essen, D-45117 Essen, Germany

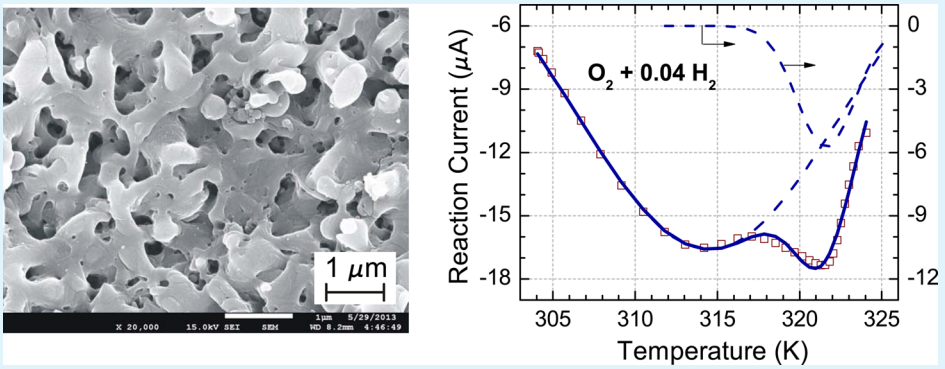

ABSTRACT: We report on the effect of temperature on the electric current induced in the mesoporous Pt/TiO_2 structure by the room temperature surface chemical reaction of hydrogen and oxygen,[13,14] which helps to unveil the physical origin of this current and the related electromotive force (chemi-EMF). We found that the temperature dependence of this reaction current has a clear multipeak structure, suggesting that at least two distinct processes contribute to the current generation. We suggest that the output current represents the interplay of both chemical and electrical processes, evidenced by the metastability of the room temperature reaction and by matching one of the current peaks with a water desorption peak for TiO_2.

KEYWORDS: *reaction current, chemicurrent, mesoporous titania, oxyhydrogen, water desorption, hydrogen spillover*

I. INTRODUCTION

Investigation of the mechanisms of generation and transport of the electrical charge in nanomaterial-based catalysts (for example, nanodispersed Pt supported on a porous TiO_2 substrate) is a key to mastering heterogeneous catalysis, control of the surface chemical reactions flow, artificial photosynthesis, and the design of advanced chemical sensors and transducers. Tuning the activity and selectivity of the catalysts through charge transfer by electrons, holes, or ions induced by external means (such as light or electric field) is a well-known and intensively studied phenomenon.[1−9]

Recent studies of the exothermic chemical reactions at the surface of nanofilm multilayer structures clearly showed that the generation and transport of the electrical charge can also occur independently of the external physical stimuli.[3,10−32] For example, the current of chemically induced energetic electrons and holes (with >0.5 eV of excess energy), known as *chemicurrent*, in Ag/Si and Cu/Si nanostructures during adsorption of atomic gas species was reported.[3,10−12] Further experiments with different gases and various thicknesses of the top electrode have shown that the magnitude of the chemicurrent is proportional to the gas flux as well as the number of empty sites on the surface, available for gas adsorption. The lifetime of chemically induced energetic electrons was shown to be on the order of tens of femtoseconds. These observations point out on an essentially nonequilibrium character of the chemicurrent generation, which, in turn, unveils an opportunity for ultrafast chemical-to-electrical signal transducers. Steady-state currents induced by catalytic oxidation of CO and H_2 species on TiO_2, SiC, and GaN Schottky structures with a continuous Pd, Pt, or Au top film were also reported.[13−19,22−25] Metal−insulator−metal structures based on metal oxide layers with thicknesses of only a few nanometers have also been used in this context.[28−30]

Recently, a different type of structure for detection of the electric current induced by a surface chemical reaction was reported.[13,14] These structures are based on mesoporous TiO_2 films grown on a Ti substrate, where an electrically continuous array of Pt nanoparticles is deposited on the TiO_2 surface. It was shown that the mesoporous Pt/TiO_2 structures allow detection of the unusually strong stationary current at room temperature when the chemical reaction rate is very slow. The origin of this current is not fully understood. Such a current induced in the mesoporous Pt/TiO_2 structure by surface chemical reactions is called the *reaction current*. As shown in ref 14, the quantum yield, the number of charge carriers detected

Received: August 2, 2013
Accepted: November 18, 2013
Published: November 20, 2013

per one H_2 molecule oxidized at the detector surface, for the mesoporous Pt/TiO_2 structures may reach 0.04 at room temperature, which is much higher than the values reported previously for the chemicurrents.[10−12,15−19,22−26] In addition to the reaction current, a significant electromotive force (open-circuit voltage) of about −0.32 V was also detected during the surface chemical reaction.[14] Large reaction currents of the reverse direction in a system with a Pt paste contact applied to the TiO_2 surface were also reported.[19]

In order to explain such a strong effect in the mesoporous Pt/TiO_2 structure, several mechanisms have been proposed for the underlying electromotive force (chemi-EMF). For example, in ref 14, the authors considered processes of proton formation at the Pt surface and their spillover into the mesoporous TiO_2 phase, where they can react with the adsorbed oxygen species to form water. The following surface reaction mechanism was suggested:

$$\text{anode (Pt):} \quad 2H \rightarrow 2H^+ + 2e^- \tag{1a}$$

$$\text{spillover:} \quad 2H^+(Pt) \rightarrow 2H^+(TiO_2) \tag{1b}$$

$$\text{cathode } (TiO_2): \quad 2H^+ + \frac{1}{2}O_2 + 2e^- \rightarrow H_2O \tag{1c}$$

Here, electrons arrive at the TiO_2 conductance band from the Pt electrode via an external electrical circuit. In ref 19, the observed chemi-EMF was also attributed to electrochemical processes similar to those observed in galvanostatic solid-electrolyte hydrogen sensors. However, the amount of experimental data available presently is insufficient either to confirm or to refute these hypotheses.

The present work unveils an *effect of temperature* on the properties of the reaction current induced in the mesoporous Pt/TiO_2 structure by oxyhydrogen reaction on its surface. We report on a complex multiregime dependence of the reaction current magnitude on the sample surface temperature, suggesting an interplay of several distinct mechanisms involved in the process of the current generation. The effects discussed in this paper can be instrumental in understanding the physical origin of the reaction current and the associated chemi-EMF.

II. SAMPLE FABRICATION AND CHARACTERIZATION

Mesoporous Pt/TiO_2 samples were fabricated in a two-step procedure, identical with the one described elsewhere.[14] First, a 10-μm-thick oxide layer was obtained on a 0.989 pure Ti metal substrate of 36 × 12 × 0.5 mm^3 dimensions using plasma electrolytic oxidation[38−40] in the 3 M sulfuric acid electrolyte. During the anodization process, the cell voltage gradually increased upon reaching 155 V, while the current was maintained constant at 0.85 A. The mesoscale porosity of the resultant TiO_2 phase is shown in Figure 1a, and its XRD spectrum was reported by these authors in ref 14. We note that fabrication of mesoporous titania using plasma electrolytic oxidation is an established technique.[38] Sul et al.[39] investigated the thickness, chemical composition, and surface morphology of TiO_2 layers grown with this method. The resultant porous structure is usually explained by a rapid motion of microdischarges along the Ti anode surface during the oxidation process.[40]

Next, a 15 nm equivalent Pt layer was deposited through a 34 × 10 mm^2 mask on one side of the anodized sample at a rate 0.02 nm/s in a 10^{-6} Torr vacuum. Subsequent field-emission scanning electron microscopy (FESEM) scans of the Pt-coated TiO_2 surface did not reveal any changes in the surface structure at the resolution of Figure 1a, implying that Pt metal was deposited as a nanometer thickness blanket layer with multiple openings (holes) at the positions of the TiO_2 surface pores (Figure 1b). We will refer to such a Pt nanophase

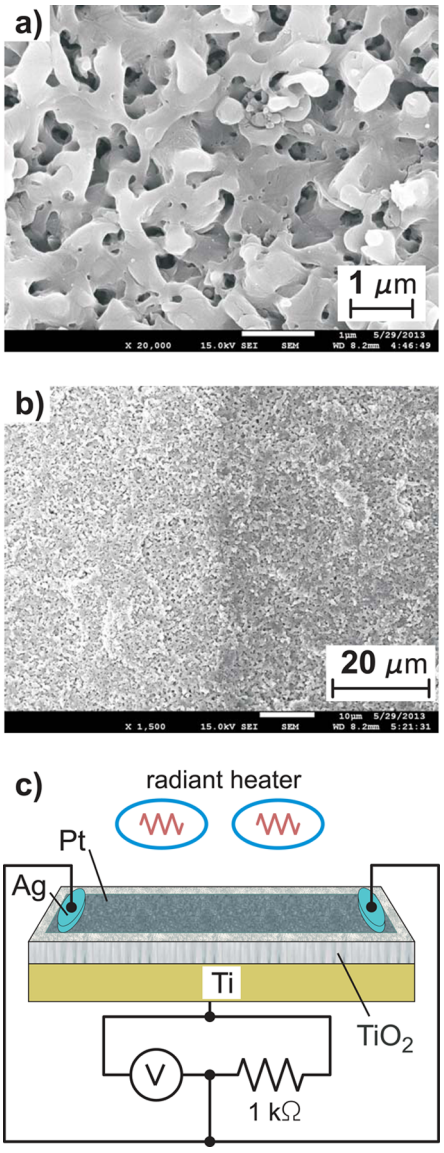

Figure 1. FESEM scans of (a) mesoporous TiO_2 phase and (b) the interface between the Pt-coated and pristine oxide surfaces. (c) Overall sample structure, reaction current measurement circuit, and heating setup.

as a "nanomesh" hereafter. The sample was then annealed at 400 K for 10−20 min, leading to a stable nanomesh resistance of 340−350 Ω measured under ambient conditions between the two Ag conductive paste terminals applied to the opposite ends of the Pt nanomesh (Figure 1c).

The sample was mounted inside a 4.5 L vacuum/environmental chamber with a base pressure of $<10^{-7}$ Torr. A small resistive temperature sensor (Omega F2020-100) was placed in the middle of the Pt-coated area of the sample. Finally, two parallel-connected halogen bulbs rated 12 V/100 W were mounted at a distance of 18 mm to the Pt-coated side of the sample to perform as a radiative heater (Figure 1c). The heater was operated at a power of less than 1.6 W per one 100 W bulb, and therefore the radiant temperatures were low enough to generate no detectable photocurrent in all experiments reported in this paper.

III. RESULTS AND DISCUSSION

Within the previous studies,[13,14] a procedure was developed that allows us a well-reproducible detection of the reaction current in the mesoporous Pt/TiO_2 structures at room

temperature. First, we initiate the ignition of hydrogen on the Pt/TiO_2 surface by adding 16 Torr H_2 to an isolated chamber with the sample assembly in a 160 Torr pure O_2 atmosphere. As can be seen from Figure 2 data, this leads to sharp reaction

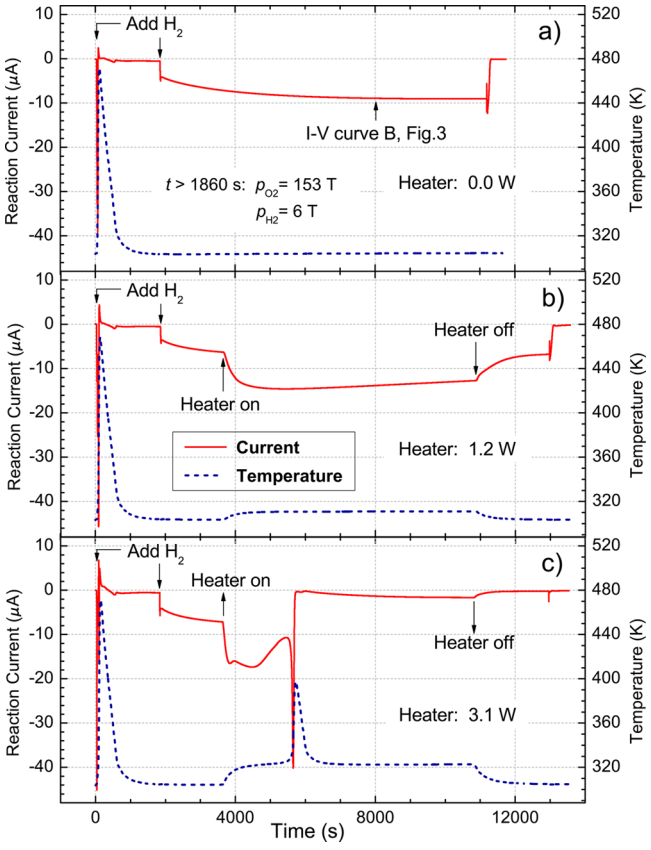

Figure 2. Long-term kinetics of the reaction current and the corresponding surface temperature reading (a) with no external heating during the entire experiment and with the radiant heater power set at (b) 1.2 W and (c) 3.1 W during the time interval 3600–10800 s. The first H_2 addition serves for activation purposes.

current and temperature peaks, which are discussed in greater detail in ref 14. We will call this process an "activation" hereafter. Presently, it is not clear what exactly happens with the surface of a mesoporous Pt/TiO_2 structure during the activation. However, we can assume that, during the activation process, the fast catalytic reaction between hydrogen and oxygen can clean the Pt/TiO_2 surface from the adsorbed residual gas particles. A similar effect was reported by Kasemo and co-workers,[33] who observed a significant increase of the catalytic activity of the Pt wire after ignition of the hydrogen and oxygen mixture occurred on its surface.

Upon completion of the transient processes by the time 900 s (Figure 2a), a small amount of H_2 about 1 Torr still remains in the chamber, the surface temperature returns to a room temperature value, and the reaction current acquires a stationary value of about 0.4 μA. This current is associated with a very slow hydrogen consumption rate, not higher than 5×10^{15} H_2 molecules per second. Interestingly, the further addition of H_2 gas to the chamber only increases the magnitude of the stationary reaction current, while the surface temperature remains unchanged. For example, admission of 5 Torr H_2 to the chamber at the time 1860 s increases the reaction current value from 0.4 to 5–9 μA during the next 2.5 h; see Figure 2a and also ref 14. The initial resistance of the Pt nanomesh (340–350 Ω) did not change significantly in the end of such an experiment, proving the long-term stability of this Pt phase.

Figure 3 shows the $I-V$ curves taken between the Ti and one of the Pt terminals (Figure 1), with a Keithley 2400

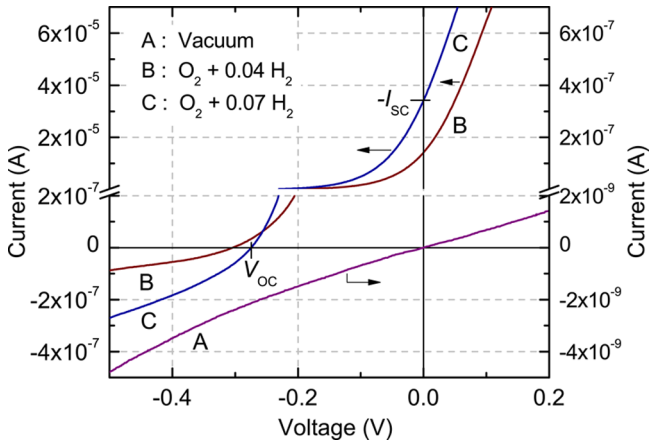

Figure 3. $I-V$ curves of the mesoporous $Pt/TiO_2/Ti$ structure measured between the Ti substrate and Pt layer (positive bias at Pt) in a vacuum (curve A), 1:0.04 oxyhydrogen mixture (curve B), and 1:0.07 oxyhydrogen mixture (curve C). The O_2 base pressure is 153 Torr in both mixtures. V_{OC} and I_{SC} are clearly defined.

sourcemeter at room temperature conditions. Linear voltage sweeps programmed from −0.7 to 0.7 V and in the reverse direction at the rate 70 mV/min were used. Such a slow rate was selected to avoid capacitive charging currents in the catalytic structure. The $I-V$ curves measured during the slow surface reaction of hydrogen and oxygen starting at the time 8000 s (see Figure 2a) differ significantly from that measured in vacuum. As seen in Figure 3, such $I-V$ curves have an asymmetric diode-like shape and intersect the I axis at the short-circuit reaction current value, I_{SC}. They also intersect the V axis at the point V_{OC}, representing the open-circuit voltage or chemical electromotive force of this structure. The values I_{SC} and V_{OC} and the overall shape of the $I-V$ curves depend on a specific composition of the oxyhydrogen mixture.

In order to study the effect of temperature on the stationary reaction current, the halogen bulb heater assembly was turned on at the time 3600 s, and a constant heater power was maintained during the time interval 3600–10800 s (Figure 2b,c). In additional experiments, which were made in a vacuum and pure oxygen, it was found that such a method of heating does not lead to generation of a measurable photocurrent. As can be seen in Figure 2b, heating of the sample in the O_2 + 0.04 H_2 gas mixture with a low power, so that the surface temperature remains below 313 K, leads only to a smooth increase of the reaction current. The current then reaches a new stationary or slowly changing value. However, when the sample is heated with a higher power (Figure 2c data), the reaction current passes through the several maxima at temperatures 314 and 321 K and then starts to decrease. Further heating initiates the ignition of hydrogen on the Pt/TiO_2 surface at a temperature of about 325 K, similar to the activation process described above.

The whole temperature dependence of the reaction current recorded in the O_2 + 0.04H_2 gas mixture for the temperature of the mesoporous Pt/TiO_2 structure in the range of 300–325 K is shown in Figure 4. The same figure also gives data for the O_2

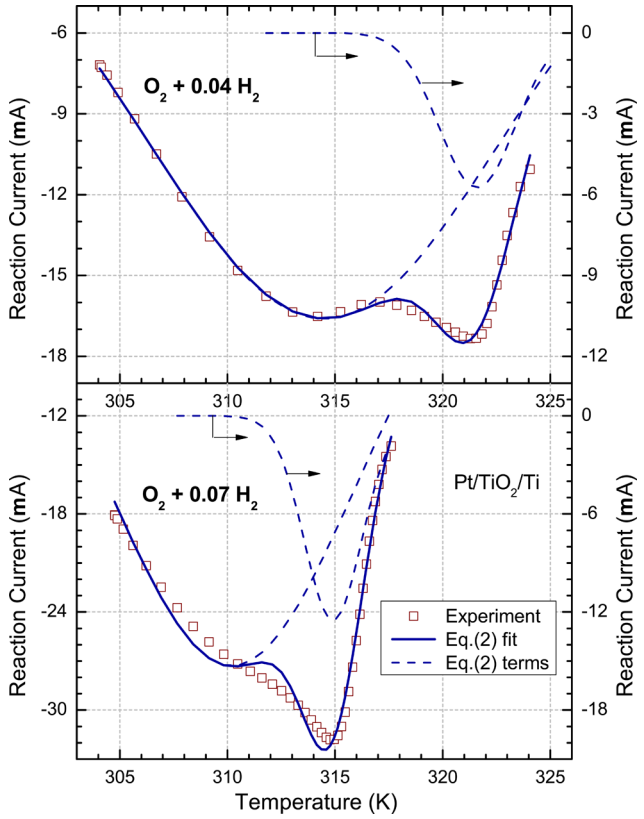

Figure 4. Temperature dependence of the stationary reaction current for the O_2 + 0.04H_2 and O_2 + 0.07H_2 mixtures at the base pressure of oxygen P_{O_2} = 153 Torr: experimental data, eq 1 analytical fit, and the constituent Gaussian peaks.

+ 0.07 H_2 gas mixture consisting of 11 Torr H_2 in 153 Torr O_2. As can be seen, in both cases the temperature dependence of the reaction current has a "W" shape with the two maxima. However, for the gas mixture with a larger hydrogen fraction, the entire temperature dependence of the reaction current shifts to higher values, while the current maxima correspond to lower temperatures.

In order to determine the exact position of the maxima, the curves of the reaction current as a function of the temperature, shown in Figure 4, have been decomposed using multiple Gaussian functions:

$$I = \sum_{i=1}^{2} A_i \exp\left[-\frac{1}{2}\left(\frac{T - T_{\max}^{(i)}}{\sigma_i}\right)^2\right] \quad (2)$$

The resulting fitting curves, as well as individual Gaussian components, are also shown in Figure 4 using thin black solid and dashed lines, respectively. Table 1 gives the parameters obtained for the Gaussian components, where T_{max} is the Kelvin temperature at the peak maximum, σ_i is the width of the peak at half-height and A_i is the peak amplitude. As can be seen, Gaussian decomposition of the reaction current as a function of temperature yields two components with the parameters dependent on the hydrogen concentration.

Table 1. Decomposition Parameters of the Temperature Dependence of an Induced Reaction Current (Data Shown in Figure 4) Using Multiple Gaussian Functions

	O_2 + 0.04H_2		O_2 + 0.07H_2	
	peak 1	peak 2	peak 1	peak 2
A (μA)	−16.6	−5.74	−27.3	−12.5
T_{max} (K)	314.5	321.6	310.2	314.9
σ (K)	8.16	1.77	5.68	1.34

Such a complex temperature dependence of the reaction current in the mesoporous Pt/TiO_2 structure can be explained as a result of the competition of several chemical and electrical processes. On the one hand, the reaction current depends on the rate of charge carrier generation in the course of a surface chemical reaction. Therefore, the temperature rise should lead to an increase in the chemical reaction rate and, consequently, stronger current. It should also be noted that the maximum of the reaction current as a function of the temperature, reported in this article, is in the same temperature range as the peak of molecular water desorption from the TiO_2 surface, which was found to be in the range of 300−350 K for disordered (powder) TiO_2 surfaces.[34] This process, in principle, could also increase the current because it leads to the cleaning of the surface from the reaction products. It could explain the first (wider) peak in the reaction temperature dependence (Figure 4), while the second peak is possibly related to the spillover process or cathode reaction activation. On the other hand, the reaction current value also depends on the properties of the charge carriers, such as lifetime and mobility, as well as the electrical properties of the Pt/TiO_2 interface. These parameters also depend on the temperature because of electron−phonon scattering processes and, as a rule, lead to a decrease in the efficiency of detection of the excited charge carriers in the diode-like structures at elevated temperatures. All of these competing factors could play a role in both Gaussian components of the reaction current.

It is interesting to note that both Gaussian components (2) have similar behavior when the hydrogen concentration is varied: they narrow and shift toward lower temperatures with a higher amount of hydrogen in the gas mixture. Also, the last point on each of the two experimental curves of Figure 4 corresponds to a heater power already sufficient to reinvoke the fast reaction process, i.e., such a mode switching occurs easier for a hydrogen-richer environment: at 315 K for the O_2 + 0.07 H_2 oxyhydrogen versus 321 K for the O_2 + 0.04 H_2 mixture. This behavior gives a hint that the system can be in a dynamic *metastable* state during the room temperature reaction. According to transition state theory,[35−37] a greater collision frequency factor related to the higher H_2 gas pressure can lead to relaxation of the metastability at a lower temperature.

IV. CONCLUSIONS

We conclude that the entire temperature dependence of the slow reaction current induced by an oxyhydrogen reaction on the mesoporous Pt/TiO_2 system[13,14] has a "W" shape with two peaks. This behavior cannot be interpreted on the basis of a *single* mechanism of the chemi-EMF, such as hot electron transport, proton spillover, or thermoelectricity.[13,14,19] Two or more distinct processes contribute to this chemi-EMF, although further studies are required for their more detailed understanding.

More generally, this reaction current represents an interplay of several chemical and electrical processes. Most notably this is evidenced (1) by the metastability of the room temperature process, which may switch to the fast mode by raising the surface temperature to only 10−20 K depending on the

hydrogen fraction in the gas phase and (2) by the matching of the reaction current peak 1, Table 1, and the water desorption peak for the titania surface.[34]

AUTHOR INFORMATION

Corresponding Author

*E-mail:ekarpov@uic.edu.

Notes

The authors declare no competing financial interest.

ACKNOWLEDGMENTS

This research is supported by U.S. National Science Foundation via Grant 1033290 and by the Center for Nanoscale Materials at Argonne National Laboratory. Use of the Center for Nanoscale Materials was supported by the U.S. Department of Energy, Office of Science, Office of Basic Energy Sciences, under Contract DE-AC02-06CH11357. I.I.N. and D.D. acknowledge the support by the German Research Foundation through the grant SFB 616.

REFERENCES

(1) Zhang, Z.; Yates, J. T. *Chem. Rev.* **2012**, *112*, 5520−5551.
(2) Gross, E.; Somorjai, G. A. *Top. Catal.* **2013**, *56*, 1049−1058.
(3) Nienhaus, H. *Surf. Sci. Rep.* **2002**, *45*, 1−78.
(4) Nowotny, M. K.; Sheppard, L. R.; Bak, T.; Nowotny, J. *J. Phys. Chem. C* **2008**, *112*, 5275−5300.
(5) Thompson, T. L.; Yates, J. T. *Chem. Rev.* **2006**, *106*, 4428−4453.
(6) Fujishima, A.; Zhang, X.; Tryk, D. A. *Surf. Sci. Rep.* **2008**, *63*, 515−582.
(7) Diebold, U. *Surf. Sci. Rep.* **2003**, *48*, 53−229.
(8) Kim, S. M.; Lee, S. J.; Kim, S. H.; Kwon, S.; Yee, K. J.; Song, H.; Somorjai, G. A.; Park, J. Y. *Nano Lett.* **2013**, *13*, 1352−1358.
(9) Kim, S. M.; Park, D.; Yuk, Y.; Kim, S. H.; Park, J. Y. *Faraday Discuss.* **2013**, *162*, 355−364.
(10) Nienhaus, H.; Bergh, H. S.; Gergen, B.; Majumdar, A.; Weinberg, W. H.; McFarland, E. W. *Appl. Phys. Lett.* **1999**, *74*, 4046−4048.
(11) Nienhaus, H.; Bergh, H. S.; Gergen, B.; Majumdar, A.; Weinberg, W. H.; McFarland, E. W. *Phys. Rev. Lett.* **1999**, *82*, 446−449.
(12) Gergen, B.; Nienhaus, H.; Weinberg, W. H.; McFarland, E. W. *Science* **2001**, *294*, 2521−2523.
(13) Karpov, E. G.; Hashemian, M. A.; Dasari, S. K. *59th AVS Annual International Symposium and Exhibition*, Tampa, FL, Oct 28−Nov 2, 2012; AVS: New York, 2012; Paper SS-MoM11.
(14) Karpov, E. G.; Hashemian, M. A.; Dasari, S. K. *J. Phys. Chem. C* **2013**, *117*, 15632−15638.
(15) Karpov, E. G.; Nedrygailov, I. I. *Appl. Phys. Lett.* **2009**, *94*, 214101.
(16) Karpov, E. G.; Nedrygailov, I. I. *Sens. Actuators B* **2010**, *148*, 388−391.
(17) Karpov, E. G.; Nedrygailov, I. I. *Proceedings of 2009 ASME 3rd International Conference on Energy Sustainability*, San Francisco, CA, July 19−23, 2009; ASME: New York, 2009.
(18) Karpov, E. G.; Nedrygailov, I. I. *Phys. Rev. B* **2010**, *81*, 205443.
(19) Schierbaum, K.; Achhab, M. E. *Phys. Status Solidi A* **2011**, *208*, 2796−2802.
(20) Bottcher, A.; Imbeck, R.; Morgante, A.; Ertl, G. *Phys. Rev. Lett.* **1990**, *65*, 2035−2037.
(21) Hellberg, L.; Stromquist, J.; Kasemo, B.; Lundqvist, B. *Phys. Rev. Lett.* **1995**, *74*, 4742−4745.
(22) Park, J.; Renzas, J.; Hsu, B.; Somorjai, G. *J. Phys. Chem. C* **2007**, *111*, 15331−15336.
(23) Park, J.; Lee, H.; Renzas, J.; Zhang, Y.; Somorjai, G. *Nano Lett.* **2008**, *8*, 2388−2392.
(24) Hervier, A.; Renzas, J. R.; Park, J. Y.; Somorjai, G. *Nano Lett.* **2009**, *9*, 3930−3933.
(25) Dasari, S.; Hashemian, M. A.; Mohan, J.; Karpov, E. G. *Chem. Phys. Lett.* **2012**, *553*, 47−50.
(26) Hashemian, M. A.; Dasari, S. K.; Karpov, E. G. *J. Vac. Sci. Technol. A* **2013**, *31*, 020603.
(27) Nedrygailov, I. I.; Karpov, E. G.; Hasselbrink, E.; Diesing, D. *J. Vac. Sci. Technol. A* **2013**, *31*, 021101.
(28) Mildner, B.; Hasselbrink, E.; Diesing, D. *Chem. Phys. Lett.* **2006**, *432*, 133−138.
(29) Schindler, B.; Diesing, D.; Hasselbrink, E. *J. Chem. Phys.* **2011**, *134*, 034705.
(30) Schindler, B.; Diesing, D.; Hasselbrink, E. *J. Phys. Chem. C* **2013**, *117*, 6337−6345.
(31) Sze, S. M. *Physics of Semiconductor Devices*, 2nd ed.; Wiley: New York, 1981.
(32) Frederikse, H. P. R. *J. Appl. Phys.* **1961**, *32*, 2211−2215.
(33) Keck, K. E.; Kasemo, B.; Hogberg, T. H. *Surf. Sci.* **1983**, *126*, 469−478.
(34) Henderson, M. A. *Surf. Sci.* **1994**, *319*, 315−328.
(35) Wigner, E. *Trans. Faraday Soc.* **1938**, *34*, 29−41.
(36) Vineyard, G. H. *J. Phys. Chem. Solids* **1957**, *3*, 121−127.
(37) Voter, A. F.; Doll, J. D. *J. Chem. Phys.* **1985**, *82*, 80−92.
(38) Diamanti, M. V.; Pedeferri, M. P. *Corros. Sci.* **2007**, *49*, 939−948.
(39) Sul, Y. T.; Johansson, C. B.; Petronis, S.; Krozer, A.; Jeong, Y.; Wennerberg, A.; Albrektsson, T. *Biomaterials* **2002**, *23*, 491−501.
(40) Park, S. J. *Met. Mater. Int.* **2008**, *14*, 449−455.